Hindawi Publishing Corporation
Journal of Nanomaterials
Volume 2012, Article ID 708519, 9 pages
doi:10.1155/2012/708519

Research Article

Phototriggered Production of Reactive Oxygen Species by TIO_2 Nanospheres and Rods

Bianca Geiseler,[1] Marko Miljevic,[1] Philipp Müller,[2] and Ljiljana Fruk[1]

[1] *DFG-Centre for Functional Nanostructures, Kalrsruhe Institute of Technology (KIT), Wolfgang-Gaede-Straße1a, 76131 Karlsruhe, Germany*
[2] *Laboratorium für Elektronmikriskopie, Karlsruhe Institute of Technology (KIT), Engessestrasse, 76131 Karlsruhe, Germany*

Correspondence should be addressed to Ljiljana Fruk, ljiljana.fruk@kit.edu

Received 5 March 2012; Revised 20 September 2012; Accepted 25 September 2012

Academic Editor: Grégory Guisbiers

We present the study of reactive oxygen species production under the light irradiation of two different types of TiO_2 nanocrystals. Both TiO_2 spheric NPs and anisotropic nanorods were investigated using activation of the horseradish peroxidase enzyme and subsequent substrate oxidation into a fluorescent product. The influence of the surface ligand dopamine was also explored to shed more light on the effect of catechol binders on the photoactivity of TiO_2 species.

1. Introduction

In recent years, anisotropic nanostructures such as nanorods, nanodiscs, cubes, or prisms [1] have started to attract more attention not only of researchers working in the field of materials science and synthetic chemistry but also biochemistry and cancer research [1–3]. Anisotropic structures have a range of properties such as large surface plasmons, which can often be tuned by changing the shape and size during the growth process [4]. Therefore, they are interesting candidates for design of different sensors, photovoltaic devices, or bioactive elements (Au rods in cancer treatment) [5, 6]. The plasmonic bands of Au nanorods, for example, can be tuned by the length of the rods, which can enable design of powerful SERS sensors or plasmonic solar cells [7–10]. Recently, they were also used as biocompatible, optically active absorbers and scatterers for targeted photodiagnostics and as contrast agents for biological imaging [11, 12]. In addition, anisotropic nanomaterials can possess different chemical affinities and therefore enable assembly of larger structures through an end-to-end binding under certain conditions [13, 14]. Furthermore, their high surface-to-volume ratio results in a high density of active surface reagents enabling further modification and improved catalytic action [15].

Titanium dioxide (TiO_2) has found numerous applications in photovoltaics [16], sensor [17] and new material design [18] and catalysis [19]. Nanoscaled semiconducting TiO_2 has also been shown to induce the production of reactive oxygen species (ROS) such as hydroxyl (OH) and peroxy (HO_2) radicals, superoxide anions (O_2^-), and hydrogen peroxide (H_2O_2) [20], upon the light irradiation in aqueous solutions, the amount depending largely on the size [21] and the morphology of the nanostructures [22]. Recently, Sayer and coworkers have shown that anatase form of TiO_2 produced more ROS species than the rutile after being exposed to the UV irradiation therefore rendering it more cytotoxic [23, 24]. Several *in vitro* studies have demonstrated that ROS produced by light triggered activation of TiO_2 nanospheres can induce oxidative damage of DNA strands [25–27]. Due to these properties, TiO_2 nanomaterials can be used for application in photodynamic cancer therapy (PDT), where the tumor cells containing TiO_2 species can be destroyed by ROS produced upon light activation [28, 29]. However, most of the ROS studies performed until now have been done using commercial Degussa P-25 and, to our knowledge, no systematic studies of the ROS production of anisotropic TiO_2 nanostructures have been reported. Furthermore, the effect of the catechol based surface binding molecules has not been explored. Herewith, we present the study and the comparison of ROS production between spherical and anisotropic rod TiO_2 as well as the influence of the bound catechol moieties onto the amount of phototriggered reactive species.

2. Experimental Section

2.1. Materials and Instrumentation. All chemicals were purchased from Sigma Aldrich and used without further purification. Horseradish peroxidase (HRP) type VI-A was used for ROS experiments. The UV/Vis absorption spectra were recorded using a CARY50 UV/Vis spectrophotometer (Agilent Technology, Germany). The TEM images were obtained on a Philips CM200 FEG/ST electron microscope. Malvern Zetasizer Nano instrument (Malvern, UK) was used to perform dynamic light scattering (DLS) and zeta potential measurements. FT-IR measurements were performed using a Bruker IFS88 FTIR-spectrometer (Bruker *Corporation*, Germany).

2.2. Synthesis of TiO_2 Nanoparticles

2.2.1. Diethylene Glycol TiO_2 Nanoparticles (TiO_2 NPdeg). TiO_2 nanoparticles were prepared using a protocol by Wang et al. with slight modification [30]. Briefly, 0.2 mL titanium(IV) chloride was added to 6 mL of DEG under vigorous stirring and inert atmosphere at 60°C. The suspension was heated at 75°C until the solution became clear. Then, 0.1 mL ddH_2O was injected into the solution and further refluxed at 160°C for 3 h. After cooling to the room temperature, 15 mL acetone was added to aid the NP precipitation. The NP solution was centrifuged and washed several times with acetone to remove residual surfactants. The average size of obtained nanoparticles, determined by TEM, was 3 nm.

2.2.2. Synthesis of Oleic Acid/Oleylamine TiO_2 Nanoparticles (TiO_2 NPole). TiO_2 nanoparticles were prepared using a protocol by Seo et al. [31] resulting in the dispersion of, in average, 3 nm TiO_2 in toluene.

2.3. Synthesis of TiO_2 Nanorods. TiO_2 nanorods (TiO_2 NR) were prepared using a protocol by Seo et al., but under different reaction times [31]. In a typical synthesis, 0.55 mL titanium(IV) chloride was added at 250°C to a solution of 3.21 mL oleic acid and 24.8 mL oleylamine. The reaction mixture was heated to 270°C under water cooling. After 2.5, 4, 6, and 8 hours, the reaction was quenched by the addition of cold toluene (6 mL) and then the reaction mixture was allowed to cool to room temperature. White or brownish TiO_2 nanorods were obtained by the addition of an excess of acetone. After centrifugation (10 min at 5000 rpm), the white powder was redissolved in 3 mL toluene and precipitated with 7 mL ethanol. These washing steps were performed three times. The nanorods were characterized by TEM.

2.4. Surface Modification of the TiO_2 NR. TiO_2 NRs (1.00 mg) were suspended in 2 mL toluene, followed by addition of 3.00 mg dopamine hydrochloride (DA) in 2 mL water. After five seconds, a color change from colorless to brown was observed indicating the formation of the charge transfer complex. The reaction mixture was further stirred overnight at 22°C. After purification by centrifugation (3x), the residue was dispersed in ddH_2O (TiO_2 NR + DA).

2.5. Radical Oxygen Species Determination. For ROS measurements, we have used an assay previously described by Fruk et al. [32] for CdS quantum dot nanoparticles, based on the activation of horse radish peroxidase (HRP) in presence of fluorogenic substrate 10-Acetyl-3,7-dihydroxyphenoxazine (Ampliflu Red). Ampliflu Red solution was prepared according to the manufacturer's instructions as a 10 mM stock in DMSO. Standard 96-well plates were used to load them with desired amounts of various TiO_2 NC. The samples were always prepared as 1 mg/mL stock solutions in KPi buffer (50 mM KH_2PO_4, 50 mM K_2HPO_4, pH = 7.0). Four different volumes were investigated (0, 1, 50, and 100 μL). When the samples were in the wells (150 μL), the plate was placed bellow the 4 W UV handheld lamp and irradiated for 30 minutes at 366 and 254 nm. The distance between the plate and the light source was 3 cm. Immediately after irradiation, HRP was added (37.6 μL, 1.33 μM) followed by addition of Ampliflu Red (10 μL, 0.9 mM). The plate was mixed in a Synergy H1 Hybrid Multi-Mode Microplate Reader for additional five minutes prior to the fluorescence measurements (λ_{ex} = 540 nm, λ_{em} = 585 nm).

2.6. Infrared Spectroscopy. FT-IR spectra of TiO_2 powders before and after ligand exchange procedures were measured.

2.7. Transmission Electron Microscopy (TEM). The TEM samples were prepared by ultrasonic dispersion of the particle solution in toluene on a carbon support film (3 nm, TED Pella Inc., California). TEM experiments were performed using a Philips CM200FEG/ST microscope. Debye diffraction patterns were analyzed using the method described in the literature [33]. The diffraction pattern of anatase and rutile were simulated using the JEMS software package.

3. Results

3.1. Synthesis and Characterization of the TiO_2 Nanorods. The nanorods were prepared using a high temperature, oleylamine-oleic acid protocol by Seo et al. [34] but introducing longer reactions time. We were interested in exploring if the prolonged reaction time has an effect of the size and the shape of the nanostructures obtained. Titanium (IV) chloride ($TiCl_4$) precursor was added to oleic acid and oleylamine, refluxed at 270°C and the morphology of prepared nanostructures was checked in regular intervals. 3 nm spherical TiO_2 NPs were obtained after 30 minutes (data not shown), but after additional reflux, only TiO_2 nanorods were present in the suspension. Samples taken after 2.5, 4, 6, and 8 hours of reflux have been imaged by TEM and it was observed that uniformly shaped NRs were obtained (Figure 1).

Mean length and widths were determined by manually measuring the dimensions of 100 rods in each sample and the data are summarized in Table 1. It can be clearly seen that 17 nm NRs are already formed after 2.5 hours and there was no significant change in length or width after the increased growth time or after the further addition of the $TiCl_4$ precursor.

These results are in slight contradiction with previously reported work by Ge et al. [35] where prolonged refluxing favored the formation of larger needle-like TiO_2 particles.

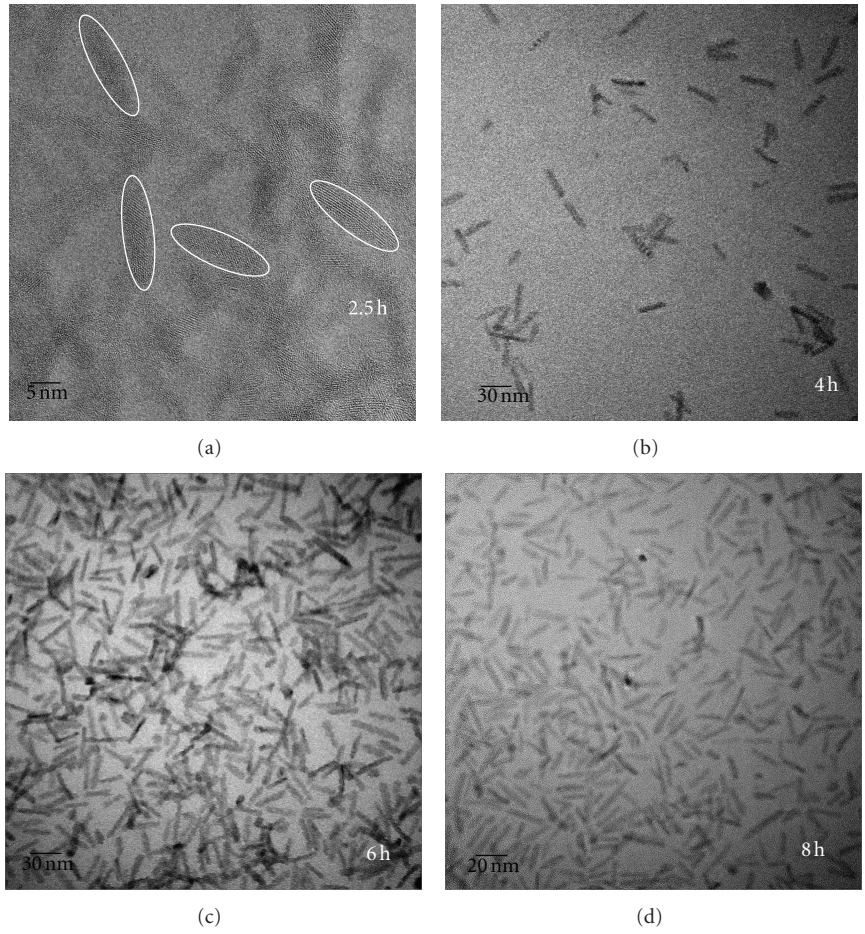

Figure 1: TEM images of TiO_2 NR obtained by oleic acid-oleylamine high-temperature method after (a) 2.5, (b) 4, (c) 6, and (d) 8 hours of reflux.

Table 1: Dimensions of produced TiO_2 nanorods using oleylamine-oleic acid protocol.

Heating period (hours)	Mean length (nm)	Mean width (nm)
2.5	17.0 ± 5.0	3.20 ± 1.2
4.0	17.0 ± 4.0	3.60 ± 0.6
6.0	17.0 ± 4.0	3.60 ± 0.6
8.0	16.0 ± 4.0	3.60 ± 0.6

However, it should be noted that we have used different solvents (oleic acid oleylamine versus water) as well as different titanium precursor ($TiCl_4$ versus $TiSO_4$), which resulted in different kinetics of the crystal growth. The crystallinity of the prepared NRs was confirmed by Debye diffraction pattern and the obtained curves were in a good agreement with the anatase form (SI, See Figure S1 in supplementary material available online at doi:10.1155/2012/708519). Prepared NRs were further characterized by UV-VIS, which showed a broad peak centered around 270 nm (Figure 2(a)).

Previous studies reported that oleic acid is able to anchor onto the surface of TiO_2 [36], but it can be easily replaced by the addition of strongly binding enediol ligands like catechols [37]. Recently, we have described the synthesis of different bifunctional dopamine (DA) based linkers, which, on one side, bind strongly onto the TiO_2 NP surface and, on the other, contain additional functional groups that enable further modification [38] and preparation of bio-friendly, aqueous suspensions of nanoparticles. For the same reasons, dopamine was used to modify the surface of the nanorods and the successful binding was determined by UV-Vis spectrometry and FT-IR spectroscopy. Catechol moieties form a strong surface charge complex with TiO_2 which results in the immediate change of color upon the addition of dopamine to TiO_2 NRs. The broad absorption peak centered around 370 nm results in excitation of an electron from the valence to the conduction band [39].

FT-IR spectra shown in Figure 3 also confirm the successful modification of TiO_2 NR surface with dopamine ligand. Above 2000 cm^{-1}, TiO_2 NR alone (Figure 3(b)) as well as TiO_2 NR + DA (Figure 3(c)) exhibit the intense antisymmetric and symmetric C-H stretching vibrations (at 2920 and 2850 cm^{-1}, resp.) of the -CH_2- groups in the hydrocarbon moiety [36]. The vibrational band of the primary amine positioned around 3300 cm^{-1} is visible in the spectrum of pure dopamine (Figure 3(a)) and also for the dopamine modified NR at 3250 cm^{-1} (TiO_2 NR + DA), which indicates that dopamine is bound to the NR surface [40]. At around

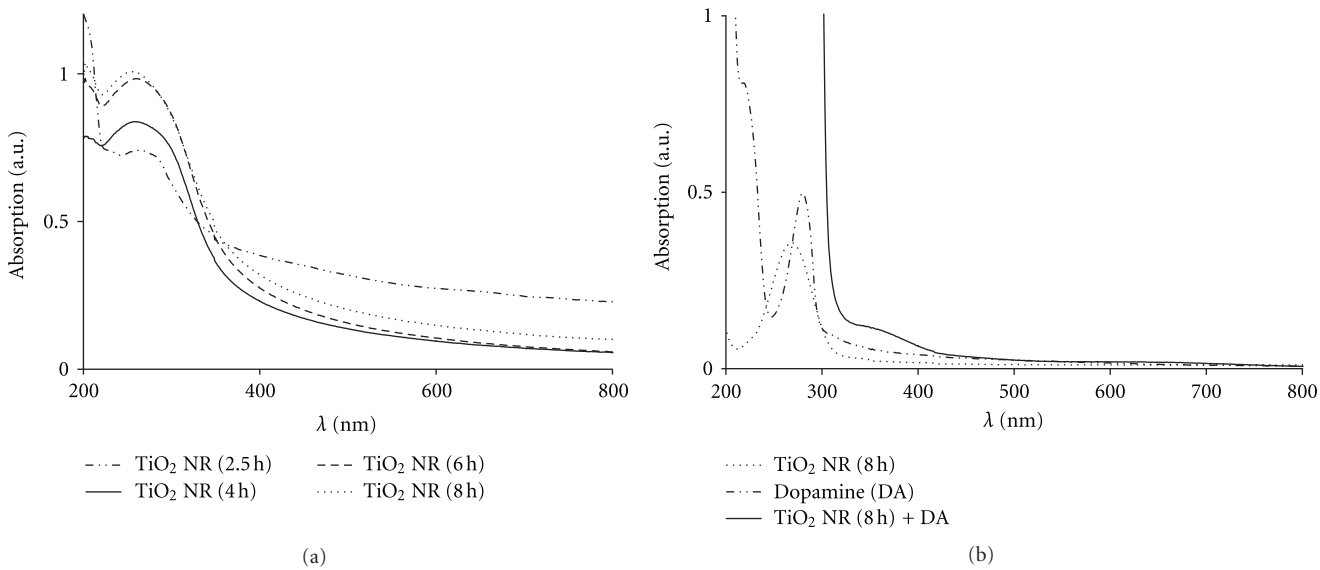

Figure 2: UV-Vis spectra of (a) TiO_2 NR synthesized by varying the reaction times and (b) after the addition of DA to TiO_2 NR (8 h).

Table 2: ζ potentials of the bare TiO_2 NRs and dopamine-modified NRs.

Heating period (hours)	Zeta average (mV) without dopamine	Zeta average (mV) modified with dopamine
2.5	13.1 ± 0.6	53.5 ± 0.8
4.0	-6.50 ± 0.1	47.7 ± 0.3
6.0	-22.5 ± 0.8	44.0 ± 1.0
8.0	-39.4 ± 0.5	38.7 ± 0.4

$1012\,cm^{-1}$, the deformation of C=CH can be observed in pure DA and also for TiO_2 NR + DA. Below $2000\,cm^{-1}$, the COO^- antisymmetric and symmetric stretching vibrations (characteristic band centered at $1454\,cm^{-1}$) of carboxylate anions [41] complexed with surface Ti centers dominate in the spectra of the oleylamine and oleic acid capped TiO_2 nanocrystals.

We have additionally characterized both unmodified and modified TiO_2 NR by measuring their ξ-potential both in prior and following dopamine (DA) functionalization and the results are summarized in Table 2.

The data show that there is a change of ξ-potential of the nanorods upon the modification. More positive zeta potential confirms that the dopamine is bound through catechol groups leaving positive amino group exposed on the surface. Interestingly, the ξ-potential of different unmodified NR becomes more negative with the time of reflux, which indicates that the amount of negative charges increases. This is probably due to the recombination of the TiO_2 species and corresponding Ti(IV) and O(II) centers on the crystal surface during the crystal growth and ripening, resulting in the change of the atom coordination [42]. The crystallinity of anatase crystals increases with the reflux time [35] resulting in the formation of basic pentacoordinated surface titanium atom and more negative surface charges.

3.2. Radical Oxygen Species Production. When a semiconductor absorbs photons with an energy greater than its band gap, electrons can be excited to the conduction band, thus creating electron-hole pairs [43]. Those excited electrons can be then recombined with the species close to the surface and it has been shown that a number of radical species can be produced in aqueous environment (Figure 4). It has been shown previously that irradiation of CdS quantum dots [32, 44] leads to the production of superoxide and hydroxyl radicals, which can recombine into H_2O_2 in aqueous solutions. Numerous enzymes are involved in H_2O_2 metabolic cycle both as a H_2O_2 generating or scavenging agents and peroxide is an important molecular fuel for triggering a range of oxidative reactions. In particular, heme containing enzymes such as peroxidases or P450 utilize H_2O_2 as an activating species to enable oxidation of a range of reactions. Not only they have important metabolic function but also have an increased application in chemical catalysis [45]. As some of the peroxidases have found applications in biosensing and catalysis, there is a number of fluorogenic substrates that can be used as peroxidase substrates and the oxidation of which results in fluorescent products in presence of H_2O_2 and the active enzyme [46].

It has been recently shown by Zhang et al. that there is a relationship between the photocatalytic activity and the surface phase [47]. The band gap of rutile was determined to be around 3.06 eV and that of anatase 3.23 eV [48] which means that UV light can be used to induce the charge separation and electron (e^-)-hole (h^+) pair generation in nanosized structures [49]. Both can recombine with the species in the proximity of the nanomaterials surface and, in aqueous solution, lead to the production of superoxide ($O_2^{-\bullet}$) and hydroxyl ($OH^\bullet$) ROS (Figure 4). These radical species can act

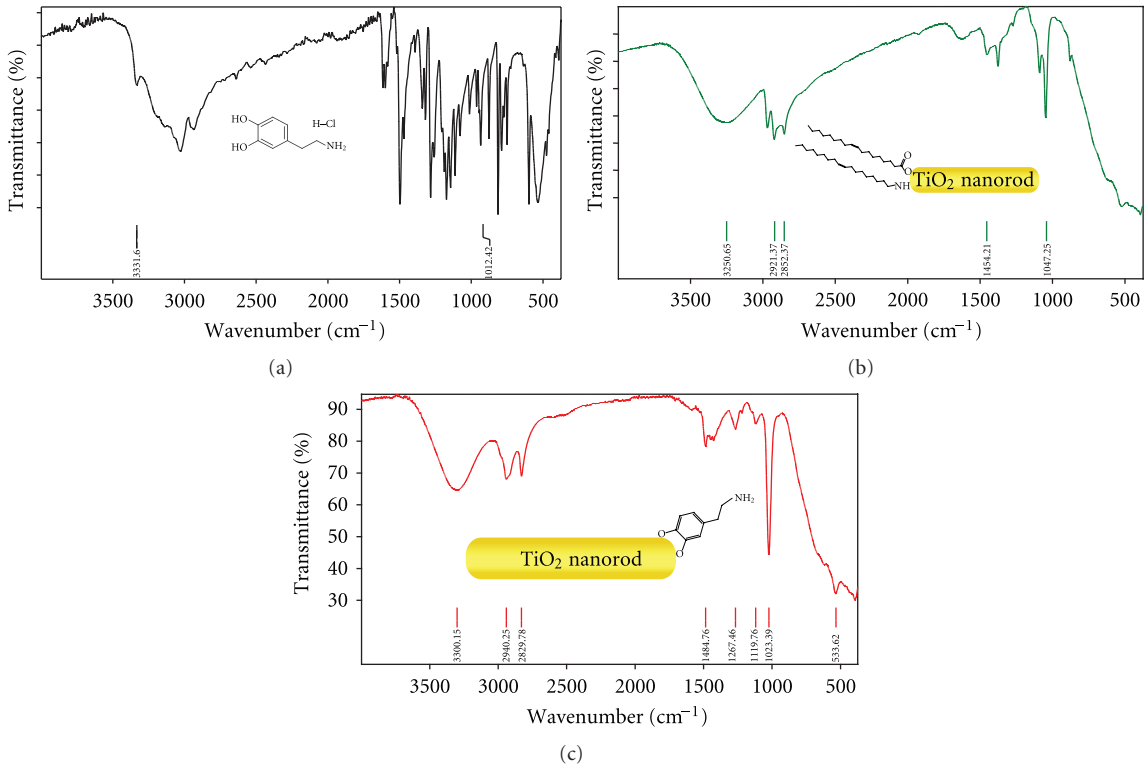

Figure 3: IR (ATR) spectra of (a) pure dopamine, (b) unmodified TiO_2 NR, and (c) TiO_2 NR + DA.

alone as heme enzyme activators [44] or could recombine into H_2O_2, which can be coordinated to the heme center and induce the cascade of reactions. The nature or the ROS species itself will be reported elsewhere as in this investigation we were interested in demonstrating that heme enzyme can be activated upon TiO_2 irradiation and the amount of activating species quantified using enzymatic assay.

To achieve this, the nonfluorescent Ampliflu Red substrate was used [50], which is oxidized by activated HRP into fluorescent resorufin. Commonly, H_2O_2 needs to be added to the enzyme solution to activate the heme center and enable the substrate oxidation. However, this can be circumvented by the addition of the semiconducting NPs, which act as light triggered generators of the activating species.

3.2.1. Activation of HRP through Irradiation of TiO_2 NPs. Oxidation of Ampliflu Red in presence of irradiated TiO_2 NPs and HRP is shown in Figure 5. To avoid any damage of Ampliflu Red and HRP that might be induced upon prolonged UV irradiation, TiO_2 NPs alone were first irradiated with 366 nm for 30 minutes and both the enzyme and the substrate subsequently added. It can be seen in Figure 5 that only in case of the commercial TiO_2 NP (TiO_2 NPcomm), significant fluorescence from the oxidized product can be observed. Both TiO_2 NPdeg and TiO_2 NPole showed small or no change. The reason for this lies in the size of the NPs—both are, on average, smaller than 5 nm. Thus, the band gap is larger [51] and requires more energy to produce electron-hole pairs, which recombine with the surrounding O_2 and H_2O molecules to generate radical species (UV-Vis SI, Figure S3). For much bigger commercial TiO_2 NPs with average diameter of 20 nm, 366 nm light is energetic enough to ensure the production of ROS species which can activate the HRP and lead to the oxidation of the substrate. More substrate is oxidized as more TiO_2 NPs is irradiated, indicating the increase of the activating species (Figure 5).

Control samples, where no NPs were added, showed no significant fluorescence. When more energetic 254 nm light source was used, increased fluorescence was observed for all three types of NPs (SI, Figure S2a). However, interestingly, in the case of TiO_2 NPdeg, which are coated with diethylene glycol, the fluorescence decreased with the increase of the TiO_2 NP concentration, indicating that there are some other effects, which play an important role in this case. We hypothesize that this is due to the degradation of ethylene glycol species upon UV irradiation with degradation products acting as radical scavengers therefore limiting the enzyme activation [52]. This effect is currently under investigation although for *in situ*, temporal control of the enzyme activation, the use of 254 nm irradiation is not desirable as it can lead to a fast degradation processes and possible deactivation of the biological molecules.

Next, dopamine coated NPs (NP + DA) were investigated to probe the influence of the surface ligands onto the ROS production. Dopamine is known to be an efficient antioxidant and it has been shown that it protects neurocytes from oxidative stress by scavenging free radicals [53]. The ROS production of dopamine depends on the concentration,

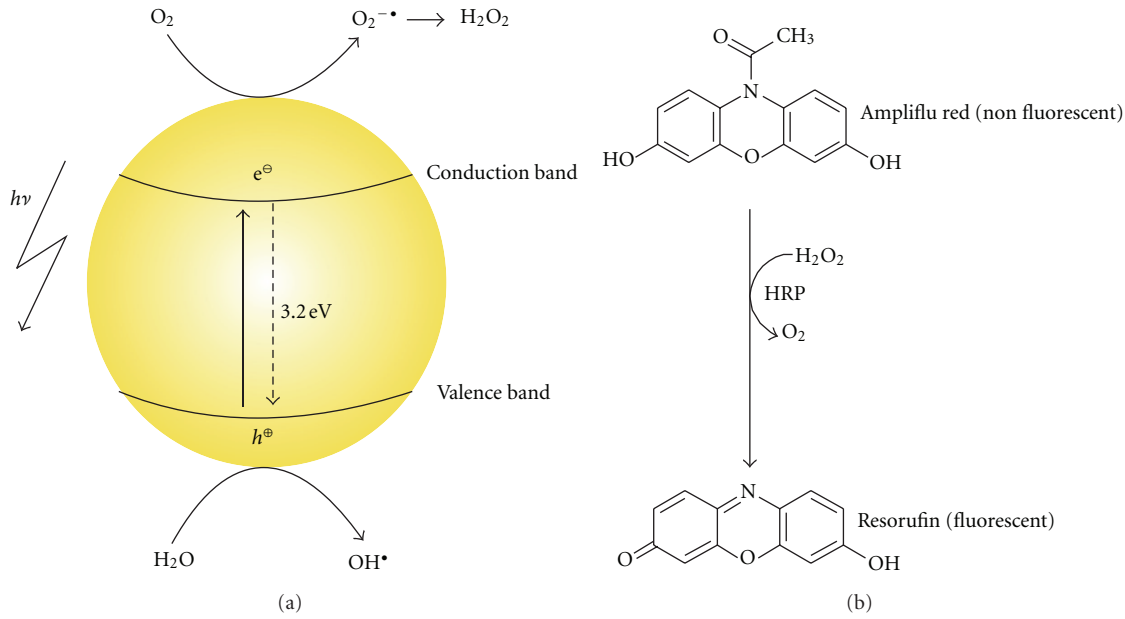

Figure 4: Generation of ROS under irradiation of semiconducting TiO_2 NP in aqueous solution and the Ampliflu activity test for HRP peroxidase.

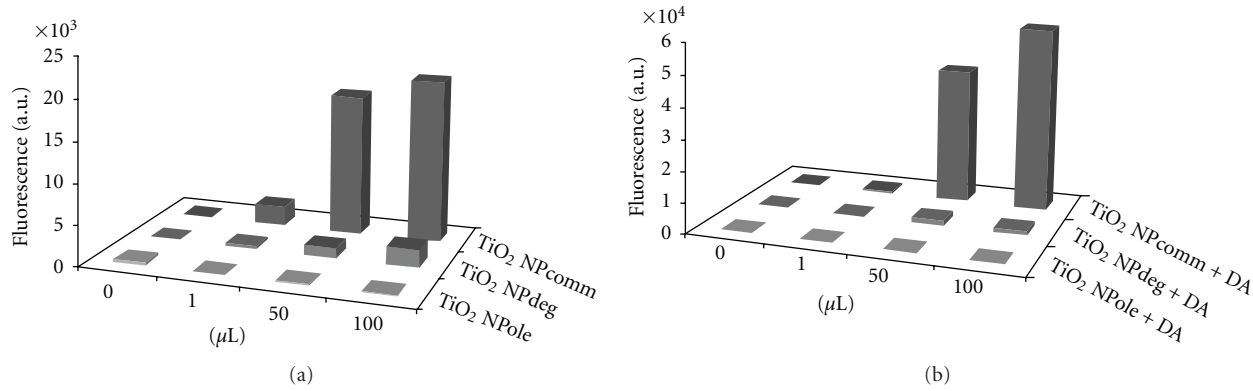

Figure 5: ROS production of three types of TiO_2 NPs: (a) TiO_2 NPcomm, and TiO_2 NPdeg, TiO_2 NPole using 366 nm light source; (b) TiO_2 NPcomm + DA, TiO_2 NPdeg + DA, and TiO_2 NPole + DA. Samples are background corrected; fluorescence of the sample kept in dark is subtracted from the fluorescence of the irradiated sample.

it can act as an antioxidant at physiologically relevant concentrations and as prooxidant at high concentrations [54]. It has been demonstrated that the generation of superoxide (O_2^{-}) and H_2O_2 can be increased when high concentrations of dopamine are used [55] and that the catechol and amine groups are the main structural features responsible for the antioxidant effect [56, 57]. Figure 5(b) shows that fluorescence intensity further increases for TiO_2 NPcomm despite the dopamine quenching ability, and there is no fluorescence in case of smaller, less active TiO_2. This result indicates that there is an apparent synergistic effect of the dopamine on the surface and NPs itself for highly active NPs probably due to the effect of the size, the ligand nature, and the charge transfer complex. The same effect was observed in case of the 254 nm light irradiation (SI, Figure S2b).

We have then explored the photo-activation of TiO_2 NRs. The activation of the HRP was successful in all of the cases although the efficiency and the fluorescence intensity increased as the TiO_2 NRs with longer reflux times were used (Figure 6(a)).

The reason for this lies in the increased crystallinity of the NRs with the reflux time. Prolonged time of crystal ripening increases the crystallinity of the rods [42] and results in less defects and higher ability to produce the ROS. The concentration dependence was also observed as the amount of the activated enzyme and the oxidized substrate increased with the increase of TiO_2 NRs concentration. We have also functionalized TiO_2 NRs with DA and compared its ROS production to the bare NRs (Figure 6(b)).

In contrast to the bare NRs, DA functionalization has a significant effect on the ROS production (Figure 6(b)). As mentioned earlier, DA is an excellent radical quencher with ability to scavenge ROS depending on the concentration. The size of the nanoobjects investigated needs to be taken into

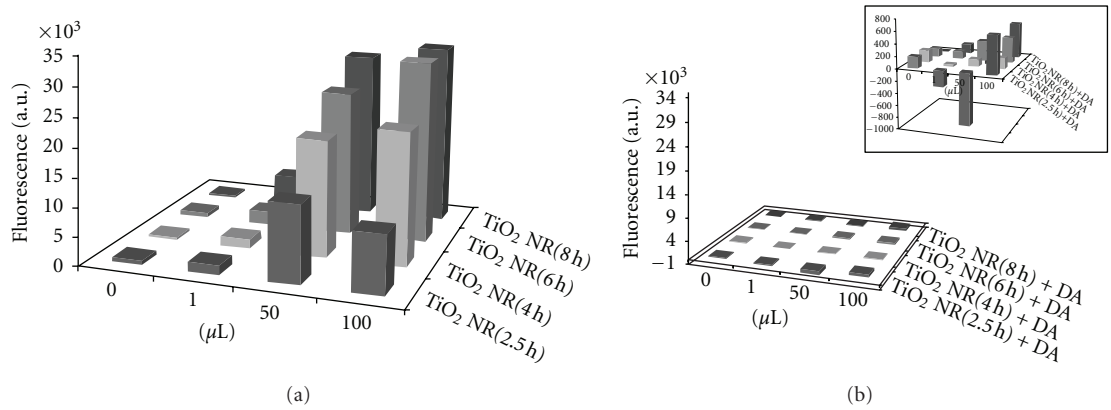

Figure 6: ROS production of four types of TiO_2 NRs: (a) bare (b) DA functionalized NRs (inset shows scale enlargement to show that there is a small activity that can be observed). Samples are background corrected; fluorescence of the sample kept in dark is subtracted from the fluorescence of the irradiated sample.

account—NRs have a larger surface available for dopamine binding. Surface area is approximately 4 times larger than that of investigated spheric NPs, which means that there is 4 times more DA that can act as an efficient dopamine scavenger. We are currently exploring other classes of catechol ligands and investigate this phenomenon.

3.2.2. Light-Induced Triggering of Peroxidase Activity Using TiO_2 NRs. As the light activation allows temporal and spatial control over the protein activity, we were interested to see if the HPR activity be switched on and off with the light irradiation to allow us to have controlled turn on activity. TiO_2 NR (8 h) where mixed with HRP and Ampliflu Red in the fluorescence quartz cuvette and the fluorescence of the resorufin measured *in situ* upon the light irradiation. The results in Figure 7 show that the activity of HRP can indeed be switched on and off with light in presence of TiO_2 NRs throughout 20 minutes. Controls in which only TiO_2 NR or HRP were used showed no such effect. This indeed indicated that such hybrid systems can be used for temporal (and spatia, i.e., in TiO_2 films) control of enzymatic activity, which could have potential applications in catalysisi and biosensing.

At the beginning of the experiment, the increase of fluorescence was observed when the light was switched on. After the initial 5 minutes, the light was switched off and the mixture kept in dark for 5 minutes during which there was no further increase of fluorescence. Fluorescence increase was restored again upon the subsequent irradiation proving that the temporal control over the enzyme activity can be achieved by addition of photoactive species.

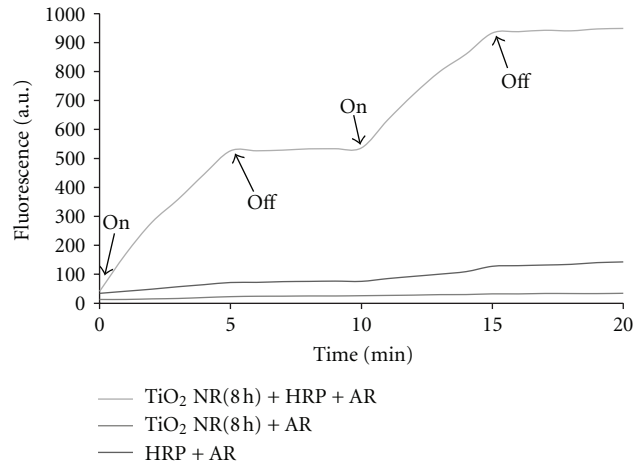

Figure 7: Light-induced triggering of peroxidase activity using TiO_2 NRs. The instances at which the light is turned on and off are labeled.

4. Conclusion

Production of enzyme activating ROS species by irradiation of different TiO_2 nanospecies was investigated. Commercially available and prepared TiO_2 spheric nanoparticles were compared to the crystalline TiO_2 nanorods. As there is a growing interest to use TiO_2 in photodynamic, therapy, it is crucial to understand the influence of the surface ligands onto the ROS production. Therefore, dopamine modified TiO_2 was studied showing that there are a significant difference between nanoparticles, which showed increased activity and nanorods, where dopamine acts as a ROS scavenger. This is an important finding, which renders dopamine undesirable in functionalization of anatase nanorods of similar dimensions, which are intended for use in ROS-related reactions. Our ongoing work is directed towards synthesis of other catechol based linkers and their effect on the phototriggered production of ROS species to aid the future design of powerful elements for photodynamic therapy.

Conflict of Interests

The authors declare they have no conflict of interests.

Acknowledgments

This work was supported by KIT Excellence Initiative 2006–2011, Grant DFG-CFN A5.7. The authors would like to thank

Dr. Vidyalakshmi Rajendran for the helpful discussions on ROS producing nanoparticles.

References

[1] E. Hao, G. C. Schatz, and J. T. Hupp, "Synthesis and optical properties of anisotropic metal nanoparticles," *Journal of Fluorescence*, vol. 14, no. 4, pp. 331–341, 2004.

[2] X. Peng, L. Manna, W. Yang et al., "Shape control of CdSe nanocrystals," *Nature*, vol. 404, pp. 59–61, 2000.

[3] Y. H. Kim, Y. W. Jun, B. H. Jun, S. M. Lee, and J. Cheon, "Sterically induced shape and crystalline phase control of GaP nanocrystals," *Journal of the American Chemical Society*, vol. 124, no. 46, pp. 13656–13657, 2002.

[4] Y. Xia, Y. Sun, Y. Wu et al., "One-dimensional nanostructures: synthesis, characterization, and applications," *Advanced Materials*, vol. 15, no. 5, pp. 353–389, 2003.

[5] Z. Wang, S. Zong, J. Yang, C. Song, J. Li, and Y. Cui, "One-step functionalized gold nanorods as intracellular probe with improved SERS performance and reduced cytotoxicity," *Biosensors and Bioelectronics*, vol. 26, no. 1, pp. 241–247, 2010.

[6] A. R. A. Loiudice, L. De Marco, M. R. Belviso, G. Caputo, P. D. Cozzoli, and G. Gigli, "Organic photovoltaic devices with colloidal TiO_2 nanorods as key functional components," *Physical Chemistry Chemical Physics*, vol. 14, pp. 3987–3995.

[7] S. E. Dobrovolskaia, "Immunological properties of engineered nanomaterials," *Nature Nanotechnology*, vol. 2, pp. 469–478, 2007.

[8] H. K. Y. Zhu, L. Xu, W. Ma et al., "Gold nanorod assembly based approach to toxin detection by SERS," *Journal of Materials Chemistry*, vol. 22, pp. 2387–2391, 2012.

[9] S. J. J. Stone and D. Wright, "Wiley interdisciplinary reviews: nanomedicine and nanobiotechnology," *Nanobiotechnology*, vol. 3, no. 1, pp. 100–109, 2011.

[10] M. P. R. Wang, L. Fruk, D. Hu, and D. M. Schaadt, "Nanoparticles and efficiency enhancement in plasmonic solar cells," *Journal of Nanoelectronics and Optoelectronics*, vol. 7, pp. 322–327.

[11] X. Huang, I. H. El-Sayed, W. Qian, and M. A. El-Sayed, "Cancer cell imaging and photothermal therapy in the near-infrared region by using gold nanorods," *Journal of the American Chemical Society*, vol. 128, no. 6, pp. 2115–2120, 2006.

[12] Q. W. L. Tong, A. Wei, and J. X. Cheng, "Gold nanorods as contrast agents for biological imaging: optical properties, surface conjugation and photothermal effects," *Photochemistry and Photobiology*, vol. 85, no. 1, pp. 21–32.

[13] C. J. Murphy, A. M. Gole, S. E. Hunyadi et al., "Chemical sensing and imaging with metallic nanorods," *Chemical Communications*, no. 5, pp. 544–557.

[14] N. M. Dimitrijevic, Z. V. Saponjic, B. M. Rabatic, and T. Rajh, "Assembly and charge transfer in hybrid TiO_2 architectures using biotin−avidin as a connector," *Journal of the American Chemical Society*, vol. 127, no. 5, pp. 1344–1345, 2005.

[15] P. D. Cozzoli, A. Kornowski, and H. Weller, "Low-temperature synthesis of soluble and processable organic-capped anatase TiO_2 Nanorods," *Journal of the American Chemical Society*, vol. 125, no. 47, pp. 14539–14548, 2003.

[16] M. Adachi, Y. Murata, J. Takao, J. Jiu, M. Sakamoto, and F. Wang, "Highly efficient dye-sensitized solar cells with a titania thin-film electrode composed of a network structure of single-crystal-like TiO_2 nanowires made by the "oriented attachmentv mechanism," *Journal of the American Chemical Society*, vol. 126, no. 45, pp. 14943–14949, 2004.

[17] Y. Zhu, J. Shi, Z. Zhang, C. Zhang, and X. Zhang, "Development of a gas sensor utilizing chemiluminescence on nano-sized titanium dioxide," *Analytical Chemistry*, vol. 74, no. 1, pp. 120–124, 2002.

[18] B. L. Bischoff and M. A. Anderson, "Peptization process in the sol-gel preparation of porous anatase (TiO_2)," *Chemistry of Materials*, vol. 7, no. 10, pp. 1772–1778, 1995.

[19] H. Y. Zhu, Y. Lan, X. P. Gao et al., "Phase transition between nanostructures of titanate and titanium dioxides via simple wet-chemical reactions," *Journal of the American Chemical Society*, vol. 127, no. 18, pp. 6730–6736, 2005.

[20] P. F. Schwarz, N. J. Turro, S. H. Bossmann, A. M. Braun, A. M. A. Abdel Wahab, and H. Dürr, "A new method to determine the generation of hydroxyl radicals in illuminated TiO_2 suspensions," *Journal of Physical Chemistry B*, vol. 101, no. 36, pp. 7127–7134, 1997.

[21] M. K. K. Matsui, M. Segawa, S. Y. Hwang, T. Tanaka, C. Ogino, and A. Kondo, "Biofunctional TiO_2 nanoparticle-mediated photokilling of cancer cells using UV irradiation," *MedChemComm*, vol. 1, no. 3, pp. 209–211, 2011.

[22] Y. Luo, Y. Tian, and Q. Rui, "Electrochemical assay of superoxide based on biomimetic enzyme at highly conductive TiO_2 nanoneedles: from principle to applications in living cells," *Chemical Communications*, no. 21, pp. 3014–3016, 2009.

[23] K. Y. K. Kakinoki, R. Teraoka, M. Otsuka, and Y. Matsuda, "Effect of relative humidity on the photocatalytic *Titanium dioxide* and photostability of famotidine," *Journal of Pharmaceutical Sciences*, vol. 93, no. 3, pp. 582–589, 2004.

[24] R. W. C. M. Sayes, P. A. Kurian, Y. Liu et al., "Correlating nanoscale titania structure with toxicity: a cytotoxicity and inflammatory response study with human dermal fibroblasts and human lung epithelial cells," *The Journal of Toxicological Sciences*, vol. 92, no. 1, pp. 174–185, 2006.

[25] J. R. Gurr, A. S. Wang, C. H. Chen, and K. Y. Jan, "Ultrafine titanium dioxide particles in the absence of photoactivation can induce oxidative damage to human bronchial epithelial cells," *Toxicology*, vol. 213, no. 1-2, pp. 66–73, 2005.

[26] H. Turkez and F. Geyikoglu, "An in vitro blood culture for evaluating the genotoxicity of titanium dioxide: the responses of antioxidant enzymes," *Toxicology and Industrial Health*, vol. 23, no. 1, pp. 19–23, 2007.

[27] J. J. Wang, B. J. Sanderson, and H. Wang, "Cyto- and genotoxicity of ultrafine TiO_2 particles in cultured human lymphoblastoid cells," *Mutation Research*, vol. 628, no. 2, pp. 99–106, 2007.

[28] T. J. Dougherty, C. J. Gomer, B. W. Henderson et al., "Photodynamic therapy," *Journal of the National Cancer Institute*, vol. 90, no. 12, pp. 889–905, 1998.

[29] Z. W. Chen and J. Zhang, "Using nanoparticles to enable simultaneous radiation and photodynamic therapies for cancer treatment," *Journal of Nanoscience and Nanotechnology,*, vol. 6, no. 4, pp. 1159–1166, 2006.

[30] P. Wang, D. Wang, H. Li, T. Xie, H. Wang, and Z. Du, "A facile solution-phase synthesis of high quality water-soluble anatase TiO_2 nanocrystals," *Journal of Colloid and Interface Science*, vol. 314, no. 1, pp. 337–340, 2007.

[31] J. W. Seo, H. Chung, M. Y. Kim, J. Lee, I. H. Choi, and J. Cheon, "Development of water-soluble single-crystalline TiO_2 nanoparticles for photocatalytic cancer-cell treatment," *Small*, vol. 3, no. 5, pp. 850–853, 2007.

[32] L. Fruk, V. Rajendran, M. Spengler, and C. M. Niemeyer, "Light-induced triggering of peroxidase activity using quantum dots," *ChemBioChem*, vol. 8, no. 18, pp. 2195–2198, 2007.

[33] C. M. C. Gammer, C. Rentenberger, and H. P. Karnthaler, "Quantitative local profile analysis of nanomaterials by electron diffraction," *Scripta Materialia*, vol. 63, no. 3, pp. 312–315, 2010.

[34] J. W. Seo, Y. W. Jun, S. J. Ko, and J. Cheon, "In situ one-pot synthesis of 1-dimensional transition metal oxide nanocrystals," *Journal of Physical Chemistry B*, vol. 109, no. 12, pp. 5389–5391, 2005.

[35] M. X. L. Ge, M. Sun, and H. Fang, "Low-temperature synthesis of photocatalytic TiO_2 thin film from aqueous anatase precursor sols," *Journal of Sol-Gel Science and Technology*, vol. 38, no. 1, pp. 47–53, 2006.

[36] P. J. Thistlethwaite and M. S. Hook, "Diffuse reflectance Fourier transform infrared study of the adsorption of oleate/oleic acid onto titania," *Langmuir*, vol. 16, no. 11, pp. 4993–4998, 2000.

[37] B. Malisova, S. Tosatti, M. Textor, K. Gademann, and S. Zürcher, "Poly(ethylene glycol) adlayers immobilized to metal oxide substrates through catechol derivatives: influence of assembly conditions on formation and stability," *Langmuir*, vol. 26, no. 6, pp. 4018–4026, 2010.

[38] B. Geiseler and L. Fruk, "Bifunctional catechol based linkers for modification of TiO_2 surfaces," *Journal of Materials Chemistry*, vol. 22, no. 2, pp. 735–741, 2012.

[39] N. M. Dimitrijevic, E. Rozhkova, and T. Rajh, "Dynamics of localized charges in dopamine-modified TiO and their effect on the formation of reactive oxygen species," *Journal of the American Chemical Society*, vol. 131, no. 8, pp. 2893–2899, 2009.

[40] M. Hesse, H. Meier, and B. Zeeh, *Spektroskopischen Methoden in der Organischen Chemie*, Stuttgart, New York, NY, USA, 1991.

[41] M. Nara, H. Torri, and M. Tasumi, "Correlation between the vibrational frequencies of the carboxylate group and the types of its coorination to a metal ion: an ab initio Molecular Orbital Study," *Journal of Physical Chemistry*, vol. 100, no. 51, pp. 19812–19817, 1999.

[42] Y. Liu, "Study of interfacial charge-transfer complex on TiO_2 particles in aqueous suspension by second-harmonic generation," *The Journal of Physical Chemistry B*, vol. 103, pp. 2480–2486, 1999.

[43] A. Fujishima and K. Honda, "Electrochemical photolysis of water at a semiconductor electrode," *Nature*, vol. 238, no. 5358, pp. 37–38, 1972.

[44] B. I. Ipe and C. M. Niemeyer, "Nanohybrids composed of quantum dots and cytochrome P450 as photocatalysts," *Angewandte Chemie International Edition*, vol. 45, no. 3, pp. 504–507, 2006.

[45] S. J. Sigg, F. Seidi, K. Renggli, T. B. Silva, G. Kali, and N. Bruns, "Horseradish peroxidase as a catalyst for atom transfer radical polymerization," *Macromolecular Rapid Communications*, vol. 32, no. 21, pp. 1710–1715, 2011.

[46] M. Tarpey, D. Wink, and M. Grisham, "Methods for detection of reactive metabolites of oxygen and nitrogen: in vitro and in vivo considerations," *American Journal of Physiology*, vol. 286, no. 3, pp. R431–R444, 2004.

[47] Q. X. J. Zhang, Z. Feng, M. Li, and C. Li, "Importance of the relationship between surface phases and photocatalytic activity of TiO_2," *Angewandte Chemie International Edition*, vol. 47, no. 9, pp. 1766–1769.

[48] A. Welte, C. W. A. Waldauf, C. Brabec, and P. J. Wellmann, "Application of optical absorbance for the investigation of electronic and structural properties of sol-gel processed TiO_2 films," *Thin Solid Films*, vol. 516, no. 20, pp. 7256–7259, 2008.

[49] Z. V. S. N. M. Dimitrijevic, B. M. Rabatic, O. G. Poluektov, and T. Rajh, "Effect of size and shape of nanocrystalline TiO_2 on photogenerated charges. An EPR study," *The Journal of Physical Chemistry C*, vol. 111, no. 40, pp. 14597–14601, 2007.

[50] K. J. Reszka, B. A. Wagner, C. P. Burns, and B. E. Britigan, "Effects of peroxidase substrates on the Amplex red/peroxidase assay: antioxidant properties of anthracyclines," *Analytical Biochemistry*, vol. 342, no. 2, pp. 327–337, 2005.

[51] N. Serpone, D. Lawless, and R. Khairutdinov, "Size effects on the photophysical properties of colloidal anatase TiO_2 particles: size quantization or direct transitions in this indirect semiconductor?" *Journal of Physical Chemistry*, vol. 99, no. 45, pp. 16646–16654, 1995.

[52] M. Suthanthiran, S. D. Solomon, and P. S. Williams, "Hydroxyl radical scavengers inhibit human natural killer cell activity," *Nature*, vol. 307, no. 5948, pp. 276–278, 1984.

[53] C. Luga, J. R. Alvarez-Idaboy, and A. Vivier-Bunge, "ROS initiated oxidation of dopamine under oxidative stress conditions in aqueous and lipidic environments," *The Journal of Physical Chemistry B*, vol. 115, no. 42, pp. 12234–12246, 2011.

[54] Z. Yang, L. D. Asico, P. Yu et al., "D5 dopamine receptor regulation of reactive oxygen species production, NADPH oxidase, and blood pressure," *American Journal of Physiology*, vol. 290, no. 1, pp. R96–R104, 2006.

[55] J. Chen, C. Wersinger, and A. Sidhu, "Chronic stimulation of D1 dopamine receptors in human SK-N-MC neuroblastoma cells induces nitric-oxide synthase activation and cytotoxicity," *Journal of Biological Chemistry*, vol. 278, no. 30, pp. 28089–28100, 2003.

[56] C. L. H and G.C. Yen, "Antioxidant effects of dopamine and related compounds," *Bioscience, Biotechnology, and Biochemistry*, vol. 61, no. 10, pp. 1646–1649, 1997.

[57] C. Luga, J. R. Alvarez-Idaboy, and A. Vivier-Bunge, "ROS initiated oxidation of dopamine under oxidative stress conditions in aqueous and lipidic environments," *The Journal of Physical Chemistry B*, vol. 115, no. 42, pp. 12234–12246, 2011.